Published in final edited form as:
Cancer Res. 2010 November 1; 70(21): 8662–8673. doi:10.1158/0008-5472.CAN-10-1435.

Cediranib/AZD2171 Inhibits Bone and Brain Metastasis in a Preclinical Model of Advanced Prostate Cancer

Juan JuanYin[1], **Luhua Zhang**[1], **Jeeva Munasinghe**[2], **Ilona Linnoila**[1], and **Kathleen Kelly**[1]

[1]Cell and Cancer Biology Branch, NCI

[2]Laboratory of Functional and Molecular Imaging and Mouse Imaging Facility, NINDS, NIH

Abstract

Late stage or aggressive cancers exhibit metastatic growth at multiple sites, and the characterization of treatment response in various organs to drugs with potentially wide-ranging efficacy is needed. Tumor cells that induce angiogenesis are a common characteristic of metastatic disease, and clinically, anti-angiogenic therapies have demonstrated value in the setting of advanced cancer. However, recent pre-clinical studies have suggested that exposure to anti-angiogenic drugs can increase tumor invasiveness and metastasis, making it important to determine in which contexts anti-angiogenic therapy is most appropriate. We describe here the effects of Cediranib, a receptor tyrosine kinase inhibitor, in a model of advanced prostate cancer metastatic to skeleton and brain. Treatment with Cediranib decreased metastatic tumor burden in the brain and bone, decreased cerebral vasogenic edema and improved survival, despite increasing the invasive histology of brain metastases. Short duration Cediranib treatment administered at the time of tumor cell dissemination was sufficient to inhibit the establishment and subsequent growth of bone metastases, although brain metastases were subject to rebound growth after the discontinuation of Cediranib. Distinct growth patterns at different organ sites in the same animal demonstrated that certain tumor microenvironments such as bone may be most amenable to interventions by anti-VEGF therapies. In addition, anti-VEGF treatment may be of utility in decreasing the rapid growth of solid brain metastases and vasogenic edema in patients with advanced cancer, leading to reduced morbidity and associated clinical benefit.

Keywords

anti-angiogenesis; metastasis; brain; bone; MRI; prostate cancer; vasogenic edema

Introduction

Metastasis is the major cause of morbidity and mortality for cancer patients. Advanced cancers frequently metastasize to distant organs, and multi-organ metastasis is not unusual (1). A common feature of metastases is vascular endothelial growth factor (VEGF) initiated angiogenesis in the tumor microenvironment (2). Anti-angiogenic therapies targeting VEGF and VEGF receptors have provided survival benefits when combined with chemotherapy for treating patients with late-stage disease, although the benefits are mostly short-lived (3). Recent pre-clinical studies have suggested that anti-angiogenic therapies increase tumor invasiveness and decrease overall survival (4,5). Although the models that have been analyzed to date are limited, the implications of such pre-clinical investigations for future clinical trial designs are

Cell and Cancer Biology Branch Center for Cancer Research, NCI 37 Convent Drive, Room 1068 Bethesda, MD 20892 301-435-4651 FAX: 301-435-4655 kellyka@mail.nih.gov .

significant. Thus, it is important to expand the range of metastasis models and to analyze various parameters of response to anti-VEGF therapies, including the tumor microenvironment context of metastatic growth in different organs. This is a consideration for assessing organ-specific risks and benefits, and especially relevant in designing therapies for treating multi-organ metastasis.

Bone and brain are common metastatic sites for breast, lung and prostate cancer as well as melanoma among others, and patients with such cancers are at risk for suffering metastases in both sites simultaneously (6,7). Brain is a well-vascularized tissue, and many of the properties expressed by tumors growing in the brain such as endothelial cell proliferation and increased vascular permeability are dependent upon VEGF (8). So far, most of the studies concerning the interactions of tumor cells and brain vasculature as well as the response of tumors to anti-VEGF therapy are evaluations of malignant gliomas (9,10). Much less data is available concerning the development of clonal brain metastases and their response to small molecule VEGFR2 inhibitors that penetrate the blood brain barrier. Similarly, relatively little is known about the vascular remodeling that occurs in developing bone metastases and the response of such metastases to anti-VEGF treatment.

The DU145 line was originally isolated from a brain metastasis of a prostate cancer patient, but the parental DU145 does not form metastases in xenograft models . Previous work has established that the introduction of an activated Ras effector mutant (RasV12G37) resulted in a gain of bone metastatic capability following intracardiac inoculation (11). To improve metastatic efficiency, the DU145(RasV12G37) cells were passaged *in vivo*, and the DU145/RasB1 cell line was isolated from a bone metastasis (12). This cell line produces high levels of VEGFA and PDGFB and metastasizes to bone and brain at a high frequency. In this study, we used Cediranib (AZD2171), a tyrosine kinase inhibitor directed against VEGFR1/2 and PDGFR, in order to determine the efficacy of various treatments and to characterize the organ-specific responses to anti-angiogenesis regimens in the setting of multi-organ metastasis.

Material and Methods

Cell culture

DU145/RasB1 cells were infected with the retrovirus pSFGnesTGL, and positive cells were isolated by FACS sorting (12).

Animal studies

Animal work was performed in accordance with a protocol approved by the NIH Animal Care and Use Committee. Intracardiac inocuation and bioluminescent imaging (BLI) were as described (12). See figure S1 for the correlation analyses between BLI and tumor burden determined histologically. For survival studies, mice were euthanized when one of the following situations applied: 10% loss of body weight, paralysis, or head tilting. All animal studies were repeated 3 times.

Experimental design

Cediranib was provided by AstraZeneca (Cheshire, UK). Cediranib was dissolved with 1% (w/v) aqueous polysorbate 80 in deionized water and given at 6mg/kg body weight, a therapeutic dose, by garvaging mice daily. To study the effect of Cediranib on mortality, morbidity and tumor progression, an experimental design as shown in Fig1A was used. Each of the four final experimental groups contained 9 or 10 animals at the initiation. For combined Cediranib and Zometa (Novartis, East Hanover, NJ) therapies, the treatments were started 3 weeks after tumor cell inoculation. To quantify osteolytic destruction, long bones were imaged with a Faxtron X-

ray machine. The numbers of hyper-intensive regions were counted for each long bone and confirmed with histology.

MR imaging

T_2 weighted axial slices, encompassing the whole brain (16 slices), were acquired using a fast spin-echo sequence to delineate anatomical details (Field-of-view (FOV)=19.2 mm, in-plane resolution=75 μm, TE/TR= 50 ms/3000 ms, echo train length=8 and NA=8, slice thickness = 1 mm, 16 slices). Quantitative T_2 weighted images of nine 1 mm axial slices (TE/TR=15/3000 ms, number of echo images =16, in-plane resolution=150 μm, inter slice gap = 1.5 mm), with the first slice positioned 1.5-mm anterior to the Bregma, were acquired. MRI data were processed and analyzed using software routines written in MATLAB (Mathworks Inc., Natic, MA).

Histology and immunohistochemistry

Brain tissue was collected and fixed in 10% buffered formalin for H&E staining or 4% paraformaldehyde for immunohistochemical staining. For morphometric analysis, each mouse brain was coronally cut into 4 equal quarters; one section from each quarter was analyzed. Mice were injected with Brdu (Sigma, St. Louis, MO, 70 mg/kg i.p) 30 min before euthanasia. The following antibodies were used: rat anti-BrdU (OBT, Oxford, United Kingdom), ApopTag in situ apoptosis detection kit (Millipore, MA), CD34 and αSMA (Abcam, Cambridge, MA). For histomorphometric analysis, bright-field microscopic images were collected using an Axioplan microscopy system (Zeiss, Thornwood, New York). Tumor cell proliferation (Brdu labeling) and apoptosis were quantified using AxioVision software (Zeiss). Histomorphometric analysis of CD34-stained vessels was performed based on previously described protocols with modifications (13). Blood vessel area was measured at 200X magnification. Co-registration of endothlial cells and pericytes was analyzed through double staining with CD34 and αSMA followed by Rhodamine and FITC conjugated secondary antibody. Fluorescent cells were counted at 400X magnification. To measure tumor invasiveness, the number of invasive edges, defined as clusters of cells outside the contour of the tumor mass, were counted for each tumor, and corrected for total tumor area. Tumors were divided into four groups based on the total area of each tumor: extra-large ($>10\times10^5\mu m^2$), large ($5\text{-}10\times10^5\mu m^2$), medium ($1.5\text{-}4.9\times10^5\mu m^2$) and small ($<1.5\times10^5\mu m^2$). Bones were decalcified in 10% EDTA for 2 weeks before processing.

Data analysis

Data were analyzed using Prizm software (GraphPad Software, Inc.) by repeated measures analysis of variance. Survival rate was analyzed by log-rank test. Data are expressed as the mean ± SE, with $P < 0.05$ considered statistically significant.

Results

1. *Cediranib* improved mortality and morbidity of tumor bearing mice

It has been previously shown that DU145/RasB1 cells form bone metastasis and highly vascularized brain metastasis following intracardiac inoculation into immunocompromised mice. Moreover, DU145/RasB1 cells secrete VEGFA, PDGFB, and angiogenin, but not angiopoietin-2, EGF, bFGF, HB-EGF, leptin or PIGF as determined by ELISA based quantibody array (Raybiotec Inc. Norcross, GA) (12). To determine the physiological response of brain and bone metastasis to anti-angiogenic therapy, mice were treated with Cediranib, a small molecule VEGF receptor antagonist that is permeable to the blood-brain barrier (9,14). A graphic depicting the experimental design is shown in Figure 1A. To determine if Cediranib inhibits the growth of established brain and bone metastasis, treatment group mice were given

Cediranib from week 3 onward when metastases can first be detected using BLI. To determine if Cediranib prevents metastatic colonization, prevention group mice were treated at the time of systemic tumor cell inoculation and thereafter for 3 weeks. Mice also were continuously treated in the prevention/treatment group from the time of tumor cell inoculation.

The effects of Cediranib treatment upon morbidity, one measure of which is body weight, and mortality were evaluated in tumor bearing mice. As shown in Figure 1B, mice in the treatment groups maintained their body weight for the study period while the mice in the control and the prevention group began losing weight at approximately 4 weeks. Consistent with this, Cediranib treatment, either continuously or starting after 3 weeks, significantly improved the survival rate of tumor bearing mice (Fig. 1C). Seventy percent of mice in the vehicle control group did not survive beyond 5 weeks, while 50% or more of mice in the treatment groups were still alive after 7 weeks. There was not a statistically significant difference between the survival of the control and prevention groups. Most mice in the control group were euthanized as a result of neurological disorders associated with edema, focal brain dysfunction secondary to multiple nodular tumors in the cerebrum and cerebellum. By contrast, Cediranib-treated mice rarely demonstrated neurological symptoms. The percentage of animals that developed metastasis is detailed in Supplemental Table 1.

2. Cediranib decreased brain metastasis burden by inhibiting solid tumor growth

Continuous treatment with Cediranib starting at the time of tumor cell dissemination resulted in significantly less brain metastatic burden after 3 weeks as measured by BLI compared with non-treated animals (Fig. 2A left panel). In the prevention arm, which encompasses treatment for the first 3 weeks after inoculation, tumor growth inhibition was maintained for the first week after discontinuation of treatment (week 4), but two weeks after the withdrawal of Cediranib (week 5), the burden of brain metastasis was similar to the untreated group, suggesting the inhibitory effects did not last (Fig.2A right panel). In the treatment arm, Cediranib inhibited the growth of established brain metastasis (Fig. 2A right panel). The inhibitory effect was obvious even after one week of treatment (week 4). At the endpoint, the brains from each experimental group were analyzed histologically in four coronal sections, distributed equally throughout the brain area. The number of mice displaying tumors and the total numer of mice evaluated as well as the absolute number of tumors observed in each experimental group are indicated in Fig. 2C. Expansive solid tumors and infiltrative tumors were observed in all regions of the brain (Fig. 2B). Solid tumors generally were larger in size than infiltrative tumors (Fig. 4B). Vehicle-treated control mice developed more solid tumors than infiltrative tumors. This proportion was reversed in Cediranib-treated mice. The treatment protocol used for the prevention group also altered the proportion of tumor types toward more invasive tumors (Fig. 2C).

To evaluate the effect of Cediranib treatment on various parameters of tumor morphology, tumors were allowed to develop for 3 weeks after tumor cell inoculation, and subsequently, mice were treated with Cediranib for 1 week. Vessel morphology was analyzed using CD34 staining (Fig. 3A). Vessels in both types of tumors appeared dilated and endothelial cells appeared hypertrophic relative to normal brain. The density of blood vessels in solid tumors in control and Cediranib-treated mice is quantified in Fig. 3B. Following Cediranib treatment, solid tumors lose blood vessel density mainly in their center while retaining a rim of vessels at the tumor border (Fig. 3A). By contrast, the vessels in infiltrative tumors were relatively insensitive to Cediranib (data not shown).

To determine the effects of drug treatment upon tumor proliferation and apoptosis, Brdu (Fig 3A) and Tunel staining (data not shown) were separately performed on serial histological sections from both control and Cediranib-treated mice. Brdu-staining demonstrated that the presence of dividing cells correlated spatially with the pattern of blood vessel density observed

upon CD34 staining. Solid tumors in the Cediranib-treated group demonstrated Brdu-labeled cells at the tumor border with significantly fewer Brdu+ cells in the body of the tumor as compared with tumors in the control group (Fig. 3A). By contrast, there were no significant differences in Brdu labeled cells for the smaller infiltrative tumors when comparing control and Cediranib-treated mice (Fig 3A). The quantification of Brdu+ cells in multiple tumors with or without 1 week of Cediranib treatment is shown in Fig. 3B. The number of apoptotic cells was not significantly increased in the Cediranib-treated mice, although some tumors from Cediranib-treated animals displayed necrotic centers (data not shown).

Because VEGF withdrawal can cause angiogenic vessels lacking pericytes to undergo regression while those stabilized by pericytes survival, we investigated whether vessel survival was correlated with co-registration of a pericyte marker (15). Endothelial cells and pericytes were co-stained for CD34 and αSMA, respectively (Fig. 3C). Approximately, 60% and 30% of vessels in solid and infiltrative tumors, respectively, stained for αSMA (Fig 3D). The reason for the reduced staining in infiltrative vessels is not known. One possibility is that a more elongated morphology of pericytes in infiltrative tumor vessels leads to the lower percentage of sectioned vessels scored as positive. Importantly, the ratio of αSMA/CD34 did not change before and after Cediranib treatment (Fig 3D). Therefore, association with αSMA did not correlate with selective survival of vessels following anti-angiogenic treatment.

Finally, an important observation for anti-angiogenic therapy is the phenotype of tumors affected by inhibition of VEGFR2 in the tumor vasculature resulting in increased tumor invasiveness. A quantitative analysis of tumors categorized with respect to tumor area and the relative density of invasive edges is shown in Figure 4B for control and mice treated with Cediranib. Although Cediranib treatment leads to fewer tumors larger than $10\times10^5\mu m^2$, those large tumors that do develop have an increased number of invasive edges (Fig. 4A). All smaller tumors have an invasive morphology and demonstrated relatively constant numbers of invasive edges between control and Cediranib-treated mice. Because the absolute numbers of small tumors did not change with treatment, it appears that the growth of newly seeded tumors was not significant during the 1 week observation period.

3. Cediranib treatment decreased vasogenic edema

Cediranib has been shown to prevent edema in glioblastoma patients, and we hypothesized that the amelioration of edema secondary to brain metastases was a factor in the improved survival of Cediranib-treated mice (9,16). To address the effects of Cediranib on vasogenic brain edema in the DU145Ras/B1 model system, BLI and MR imaging were used between 3.5-4.5 weeks after the initiation of experimental metastasis to evaluate tumor burden, anatomical structures and edema. Tumor-bearing mice without evidence of significant edema were randomized to control and Cediranib-treated groups. After 7 days, 5 control and 3 treated mice were re-imaged. As shown by a representative example in Fig. 5A and quantified in 5B, the T2 maps showed accumulation of edema in the control mice along the white matter tracts of the brain. The animals treated with Cediranib, however, showed no discernable difference in T2 values after one week, even though the morphology scans demonstrated an increase in tumor diameter during the study period (Fig. 5A&B). The prevention of edema by Cediranib was confirmed by luxol fast blue staining for myelin in histological sections from control and treated mouse brains (Fig. 5C). Demyelination, which is indicative of edema, was seen along the corpus callosum of control mice, matching the hyperintensive areas in the T2 maps (Fig. 5A).

To test whether Cediranib can ameliorate established edema, 3 tumor-bearing mice with radiological evidence of edema were treated with Cediranib for 7 days. Control mice were not included in this arm as they would not survive for an additional 7 days with established brain edema. Cediranib-treated mice survived without significant morbidity to the second scan date,

which revealed stabilization or reduction of edema, despite expansion of the metastatic lesions as revealed by morphology scans (Fig. 5D).

4. Cediranib inhibited bone metastasis even after short duration treatment

There has been relatively little preclinical evaluation of the effects of anti-angiogenic agents on the development and progression of bone metastases. Intracardiac inoculation of DU145/RasB1 cells leads to osteolytic bone metastases, and BLI of the long bones and spine was assessed in the four groups shown in Fig. 1A. The inhibition of bone metastatic growth was evident after two and three weeks of continuous treatment (Fig. 6A left). In the prevention group, bone metastasis did not relapse at week 5, following withdrawal of Cediranib at week 3 (Fig.6A right). This contrasts with the renewed growth of brain metastasis at this same time point. Also, treatment of established bone metastasis either continuously from their initiation or starting at week 4 onward, inhibited BLI at least 10-fold (Fig. 6A right). The BLI data were confirmed with histomorphometric analysis of bone sections (Fig. 6B) and X-rays (not shown).

Bone metastases were stained for CD34 to determine the effect of Cediranib on vessel number and morphology (Fig. 6C&D). Non-treated mice displayed a uniform high density of CD34+ vessels within bone metastases, and many vessels appeared dilated. The vessel density as well as the dilated appearance decreased in bone metastases from Cediranib-treated animals. The vessel area relative to total tumor area decreased approximately six fold as a result of Cediranib treatment (Fig. 6D).

VEGF-A binding to VEGFR1 has been shown to stimulate osteoclast differentiation, migration, and activity (17). Because Cediranib has some inhibitory activity for VEGFR1 (14), the osteoclast number/mm normal bone or per tumor bone interface was quantified in non-tumor bearing and tumor-bearing mice, respectively, either untreated for 4 weeks or Cediranib-treated between weeks 3 and 4. In non-tumor bearing mice, Cediranib did not affect osteoclast number (Supplement Fig. 2). Although Cediranib-treated mice developed smaller and fewer bone metastases, the osteoclast number per mm tumor bone interface was not affected.

Bisphosphonates, such as Zometa are currently used for a variety of patients with metastatic bone lesions, including lesions originating from prostate cancer (18). Because Cediranib did not appear to inhibit osteoclast activity, the effects of Cediranib and Zometa were directly compared as monotherapy agents and as potentially synergistic drugs in combination. BLI revealed that continuous treatment from the time of tumor cell inoculation with Cediranib, Zometa, and a combination of both drugs inhibited tumor burden significantly and approximately equally (Fig. 7A). Histopathologic analyses of bone sections demonstrated that there were fewer bone metastases in Cediranib-treated mice as compared to controls, and those metastases that did develop were generally smaller. The bone metastases growing in the presence of Zometa showed metaphyseal sclerosis with tumor cells embedded in the trabecular bone (Fig. 7B). Consistent with the histological analysis, Zometa treatment resulted in almost complete inhibition of radiologically evident osteolytic lesions (Fig. 7C). Parallel BLI of the brain at 5 weeks showed that Zometa alone had no statistically significant effect upon the brain metastatic burden (Fig. 7D).

Discussion

We investigated the efficacy of various Cediranib prevention and treatment regimens, using an experimental model of hematogenously-disseminated prostate cancer that metastasizes predominantly to brain and bone. This system models critical steps in metastatic spread including dissemination, extravasation, and colonization of selected prostate cancer cells. The DU145/RasB1 model is specifically useful as brain and bone are major sites of metastasis for

many commonly-occurring cancers, and co-occurrence at the two sites is not unusual (7,8). Cediranib treatment starting either from the time of DU145/RasB1 intracardiac inoculation or starting after the establishment of micrometastases led to a significant survival benefit that correlated with decreased tumor burden and decreased cerebral vasogenic edema.

The response of brain metastases to Cediranib was multifaceted and displayed distinct histologic features. Untreated mice were more likely to develop rapidly-growing and expansive solid brain metastases, which contributed to most of the brain tumor burden, while the occurrence of small invasive tumors was relatively rare. Cediranib treatment led to regression of the vessels in the center of large tumors. By contrast, neither the tumor vasculature of the invasive tumors nor the tumor cells at the rim of the large expansive tumors regressed after Cediranib treatment. The perivasular pattern of growth following anti-angiogenic treatment was characteristic of vessel co-option, which has been observed also for glioblastoma and melanoma (19,20).

Preclinical models have implications for understanding both the mechanisms of treatment response and resistance as well as potential morbidity and mortality benefits. Outside of glioblastoma, there are limited examples analyzing the response of tumor cells in the brain to anti-angiogenic treatment. Kim et al. described the response of MDA-231 breast cancer brain metastases to PTK 787, resulting in decreased tumor burden but no obvious survival benefit (21). Vessel co-option was not specifically addressed. Leenders et al. assessed the response of cerebral melanoma metastases to ZD6474 where a decreased tumor burden, no survival benefit, and evidence of vessel cooption were observed (22). The preclinical model presented here adds to the small body of data showing that vessel cooption is a general response of different cell types to anti-angiogenic treatment in the highly-vascularized brain microenvironment.

Vessel co-option following treatment may represent strong selective pressure upon the propensity of tumor cells in the brain to colonize pre-existing vessels as a result of their adhesion to the vascular basement membrane (23). In the DU145/RasB1 model, a morphological difference was not apparent to explain the sensitivity of endothelial cell survival in the co-opting versus solid tumors. The vasculature in both expansive and invasive tumors appeared dilated, and there did not appear to be a selective survival of vessels with demonstrably different pericyte coverage following anti-angiogenic treatment. The lack of response of the perivascular brain metastases seen here is consistent with a limited amount of imaging data from clinical trials suggesting increased infiltrative growth in advanced glioblastoma treated with bevacizumab (10). Increasing long-term survival in patients with brain metastasis may require combination therapies to inhibit several functions including adhesion between tumor cells and cerebral vessels, infiltrative growth and angiogenesis. However, for palliative therapy, it seems likely that Cediranib treatment will be useful for mitigating the morbidity associated with progressive brain metastasis, similar to the situation with advanced glioblastoma (9).

Recent attention has focused upon observations from genetically engineered mouse tumor and experimental metastasis models showing that inhibition of the VEGF/VEGFR2 axis leads to increased tumor invasiveness and micrometastasis formation (4,5). Consistent with these studies, histological analyses of established DU145/RasB1 brain metastases revealed increased invasive projections after 1 week of Cediranib treatment, which were most apparent in the largest tumors. On the other hand, increased survival and decreased metastatic tumor burden in DU145/RasB1 inoculated mice treated continuously with Cediranib contrasts with the results of Ebos and colleagues (4). In the Ebos experimental design, Sunitinib treatment accelerated metastatic burden and decreased over-all survival in mice following introduction of MB-MDA-231 breast cancer cells via tail vein injection or following removal of primary orthotopically grown tumors. It is likely that these contrasting endpoints are in-part a result of

tumor-specific contributions. In addition, we suggest that the tumor microenvironment in various organs will be differently affected by anti-angiogenic treatments. Specifically, it appears that the major site of metastatic burden was the lungs in the Ebos studies with MB-MDA-231. The lungs may be most susceptible to "metastatic conditioning," which is thought to reflect circumstances that increase tumor cell extravasation and initial colonization, such as in response to stress/injury, including anti-angiogenic treatment (4,24).

An interesting observation to emerge from our studies is the different sensitivity of brain or bone resident tumor cells to Cediranib treatment and subsequent withdrawal. After 3 weeks of Cediranib treatment from the time of tumor cell dissemination, Cediranib withdrawal led to rebound growth of brain metastases, while bone metastases were significantly inhibited. Thus, individual or micrometastatic tumor cells in the bone as compared to the brain appeared to either not survive a VEGF signaling deficient microenvironment, or alternatively, were not able to emerge from dormancy after Cediranib withdrawal.

One interpretation of these results is that tumor-initiating cell niches in the brain and bone microenvironment are affected differently by inhibition of the VEGF axis. The source of such differential effects could be differences in the endothelial cells themselves as well as the differentiated cells making up the parenchyma of the organ (25). Vascular niches that contribute to the survival and establishment of glioma-initiating cells (GIC) in the brain and leukemia-initiating cells (LIC) in the bone marrow have been described (26,27). An alternative interpretation is that Cediranib directly disrupts osteogenic cells involved in bone remodeling through effects upon VEGFR1 expressed hematopoietic cells, such as osteoclasts. However, we found no evidence for functional effects of Cediranib on osteoclasts in control or tumor-bearing mice. Thus, we favor the interpretation that at the dosage used in this study, Cediranib influences the growth of bone metastasis via an effect upon VEGFR2 and bone endothelium.

In summary, our work provides evidence that antiangiogenic treatment not only inhibited the growth of aggressive prostate cancer metastases in bone and brain, but also reduced the morbidity and mortality of tumor bearing mice. These results support a value for clinical trials investigating appropriate combination therapies that include anti-angiogenic drugs for treatment of patients with advanced cancer.

Supplementary Material

Refer to Web version on PubMed Central for supplementary material.

Acknowledgments

This research was supported by the Intramural Research Program of the NIH, National Cancer Institute, Center for Cancer Research.

References

1. Chambers AF, Groom AC, MacDonald IC. Dissemination and growth of cancer cells in metastatic sites. Nat Rev Cancer 2002;2:563–72. [PubMed: 12154349]
2. Ellis LM, Hicklin DJ. VEGF-targeted therapy: mechanisms of anti-tumour activity. Nat Rev Cancer 2008;8:579–91. [PubMed: 18596824]
3. Loges S, Mazzone M, Hohensinner P, Carmeliet P. Silencing or fueling metastasis with VEGF inhibitors: antiangiogenesis revisited. Cancer Cell 2009;15:167–70. [PubMed: 19249675]
4. Ebos JM, Lee CR, Cruz-Munoz W, Bjarnason GA, Christensen JG, Kerbel RS. Accelerated metastasis after short-term treatment with a potent inhibitor of tumor angiogenesis. Cancer Cell 2009;15:232–9. [PubMed: 19249681]

5. Paez-Ribes M, Allen E, Hudock J, et al. Antiangiogenic therapy elicits malignant progression of tumors to increased local invasion and distant metastasis. Cancer Cell 2009;15:220–31. [PubMed: 19249680]
6. Kingsley LA, Fournier PG, Chirgwin JM, Guise TA. Molecular biology of bone metastasis. Mol Cancer Ther 2007;6:2609–17. [PubMed: 17938257]
7. Palmieri D, Chambers AF, Felding-Habermann B, Huang S, Steeg PS. The biology of metastasis to a sanctuary site. Clin Cancer Res 2007;13:1656–62. [PubMed: 17363518]
8. Jain RK, di Tomaso E, Duda DG, Loeffler JS, Sorensen AG, Batchelor TT. Angiogenesis in brain tumours. Nat Rev Neurosci 2007;8:610–22. [PubMed: 17643088]
9. Batchelor TT, Sorensen AG, di Tomaso E, et al. AZD2171, a pan-VEGF receptor tyrosine kinase inhibitor, normalizes tumor vasculature and alleviates edema in glioblastoma patients. Cancer Cell 2007;11:83–95. [PubMed: 17222792]
10. Narayana A, Kelly P, Golfinos J, et al. Antiangiogenic therapy using bevacizumab in recurrent high-grade glioma: impact on local control and patient survival. J Neurosurg 2009;110:173–80. [PubMed: 18834263]
11. Yin J, Pollock C, Tracy K, et al. Activation of the RalGEF/Ral pathway promotes prostate cancer metastasis to bone. Mol Cell Biol 2007;27:7538–50. [PubMed: 17709381]
12. JuanYin J, Tracy K, Zhang L, et al. Noninvasive imaging of the functional effects of anti-VEGF therapy on tumor cell extravasation and regional blood volume in an experimental brain metastasis model. Clin Exp Metastasis 2009;26:403–14. [PubMed: 19277878]
13. Lavazza C, Carlo-Stella C, Giacomini A, et al. Human CD34+ cells engineered to express membrane-bound tumor necrosis factor-related apoptosis-inducing ligand target both tumor cells and tumor vasculature. Blood 115:2231–40. [PubMed: 20075160]
14. Wedge SR, Kendrew J, Hennequin LF, et al. AZD2171: a highly potent, orally bioavailable, vascular endothelial growth factor receptor-2 tyrosine kinase inhibitor for the treatment of cancer. Cancer Res 2005;65:4389–400. [PubMed: 15899831]
15. Bergers G, Song S, Meyer-Morse N, Bergsland E, Hanahan D. Benefits of targeting both pericytes and endothelial cells in the tumor vasculature with kinase inhibitors. J Clin Invest 2003;111:1287–95. [PubMed: 12727920]
16. Gerstner ER, Duda DG, di Tomaso E, et al. VEGF inhibitors in the treatment of cerebral edema in patients with brain cancer. Nat Rev Clin Oncol 2009;6:229–36. [PubMed: 19333229]
17. Aldridge SE, Lennard TW, Williams JR, Birch MA. Vascular endothelial growth factor receptors in osteoclast differentiation and function. Biochem Biophys Res Commun 2005;335:793–8. [PubMed: 16105658]
18. Aapro M, Abrahamsson PA, Body JJ, et al. Guidance on the use of bisphosphonates in solid tumours: recommendations of an international expert panel. Ann Oncol 2008;19:420–32. [PubMed: 17906299]
19. Bergers G, Hanahan D. Modes of resistance to anti-angiogenic therapy. Nat Rev Cancer 2008;8:592–603. [PubMed: 18650835]
20. Rubenstein JL, Kim J, Ozawa T, et al. Anti-VEGF antibody treatment of glioblastoma prolongs survival but results in increased vascular cooption. Neoplasia 2000;2:306–14. [PubMed: 11005565]
21. Kim LS, Huang S, Lu W, Lev DC, Price JE. Vascular endothelial growth factor expression promotes the growth of breast cancer brain metastases in nude mice. Clin Exp Metastasis 2004;21:107–18. [PubMed: 15168728]
22. Leenders WP, Kusters B, Verrijp K, et al. Antiangiogenic therapy of cerebral melanoma metastases results in sustained tumor progression via vessel co-option. Clin Cancer Res 2004;10:6222–30. [PubMed: 15448011]
23. Carbonell WS, Ansorge O, Sibson N, Muschel R. The vascular basement membrane as “soil” in brain metastasis. PLoS One 2009;4:e5857. [PubMed: 19516901]
24. Bidard FC, Pierga JY, Vincent-Salomon A, Poupon MF. A “class action” against the microenvironment: do cancer cells cooperate in metastasis? Cancer Metastasis Rev 2008;27:5–10. [PubMed: 18066649]
25. Aird WC. Phenotypic heterogeneity of the endothelium: I. Structure, function, and mechanisms. Circ Res 2007;100:158–73. [PubMed: 17272818]
26. Calabrese C, Poppleton H, Kocak M, et al. A perivascular niche for brain tumor stem cells. Cancer Cell 2007;11:69–82. [PubMed: 17222791]

27. Lane SW, Scadden DT, Gilliland DG. The leukemic stem cell niche: current concepts and therapeutic opportunities. Blood 2009;114:1150–7. [PubMed: 19401558]

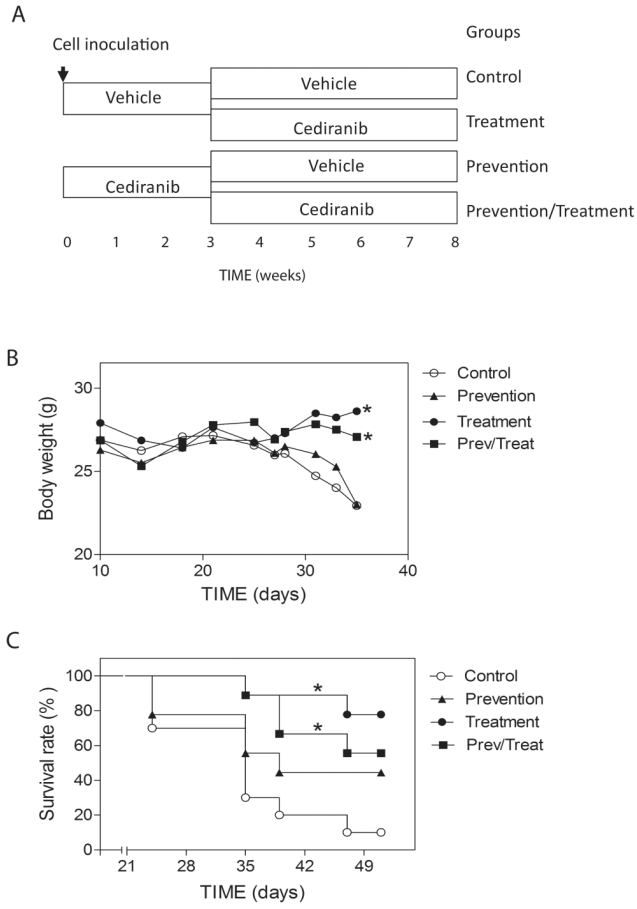

Figure 1.

Cediranib decreased mortality and morbidity of tumor bearing mice. A. Experimental design for Cediranib treatment. Cells were inoculated at day 0. Mice were treated with vehicle or Cediranib for the first three weeks (n=20 per group), and subsequently both groups were randomly divided into two groups. One group was treated with vehicle and the other group was treated with Cediranib, (n=9-10). B. Body weight change of tumor-bearing mice in different groups.* $p<0.001$. C. Survival rate of tumor-bearing mice in each group.* $p<0.05$.

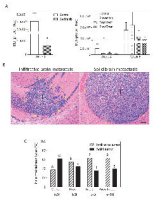

Figure 2.

Cediranib inhibited the development and progression of brain metastasis. A. Brain tumor burden measured by BLI at weeks 3 (left panel), 4 and 5 (right panel) in different groups (n=9-10), * $p<0.05$. B. Representative histological images of infiltrative (left panel) and solid type (right panel) brain metastasis. T: tumor. Scale bar=100μm. Yellow arrows indicate tumor regions. C. Percentage of infiltrative and solid tumor types quantified on histological sections of brain in each group. The numbers above each column represent the total number of specific histological types of brain metastases. The ratio below the graph is the incidence of brain metastasis in each group.

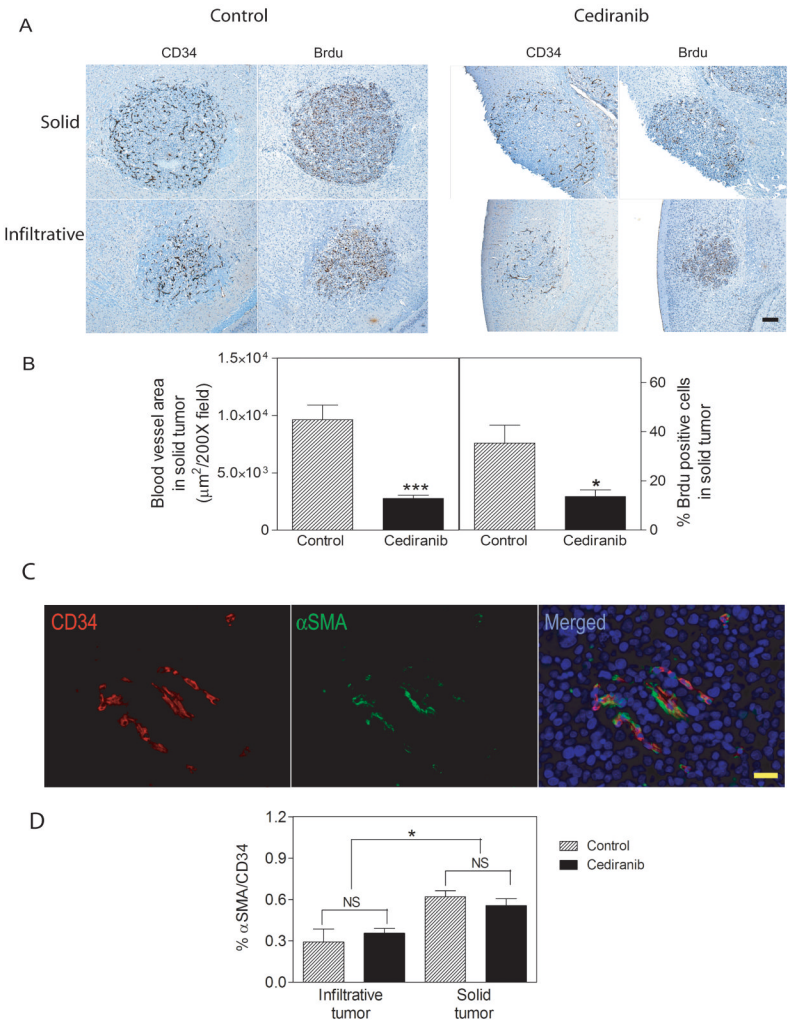

Figure 3.

The effects of Cediranib on tumor blood vessel density and tumor cell proliferation. A. CD34 positive endothelial cells and Brdu positive proliferating cells in consecutive sections of brain metastases from a control (left panels) and Cediranib treated (right panels) mice. The upper panels show large solid tumors and the lower panels show infiltrative tumors. Scale bar=100μm. C. Blood vessel areas (left panel, n=12) and Brdu positive cells (right panel) were quantified in solid brain tumors from control and Cediranib treated group. C. Representative double stain images for CD34 positive endothelia cells in red (left panel) and αSMA positive pericytes in green (middle panel) in a solid tumor. Right panel shows merged image. Scale bar=20μm. D. Quantification of the ratio of αSMA and CD34 positive blood vessels in solid and infiltrative tumors. * $p<0.05$.

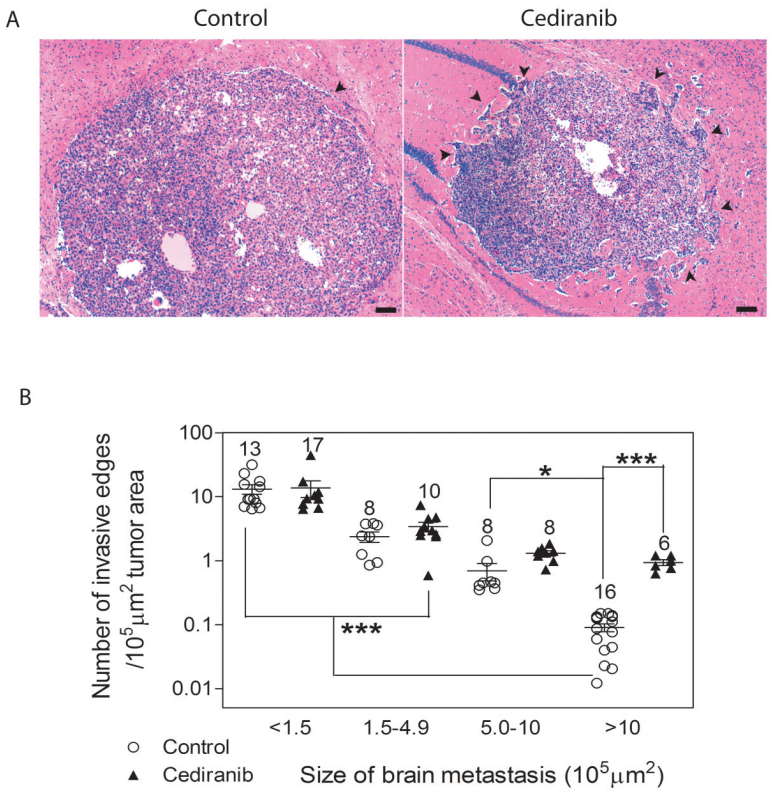

Figure 4.

Cediranib treatment affects the invasiveness in larger tumors. A. Representative images of larger brain metastases from a control (left panel) and Cediranib treated (right panel) mice. Black arrows indicate invasive edges. Scale bar=100μm. B. Quantification of the number of invasive edges for tumors of various areas. The absolute numbers of tumors quantified are indicated above the data points. * $p<0.05$, *** $p<0.001$.

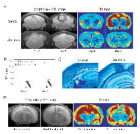

Figure 5.

Cediranib inhibited the development and progression of brain edema in tumor bearing mice. A. T2 scans (left four panels) and T2 maps (right four panels) of brains in control (upper panels) and Cediranib-treated (lower panels) mice. Mice were treated for one week when brain metastases were obvious by BLI and before edema developed. Red arrows indicate brain metastasis. B. Quantification of brain edema using T2 values from 4A. C. Luxol fast blue stain of mouse brains show separation of myelin (red arrow) in control brain, while myelin remains intact in Cediranib-treated brain (yellow arrow). Scale bar=200μm. T: tumor. D. Representative T2 scans (left two panels) and T2 maps (right two panels) of brains pre- and post- Cediranib treatment. Cediranib was adminstrated after brain edema had developed. n=3, arrows indicate brain metastasis.

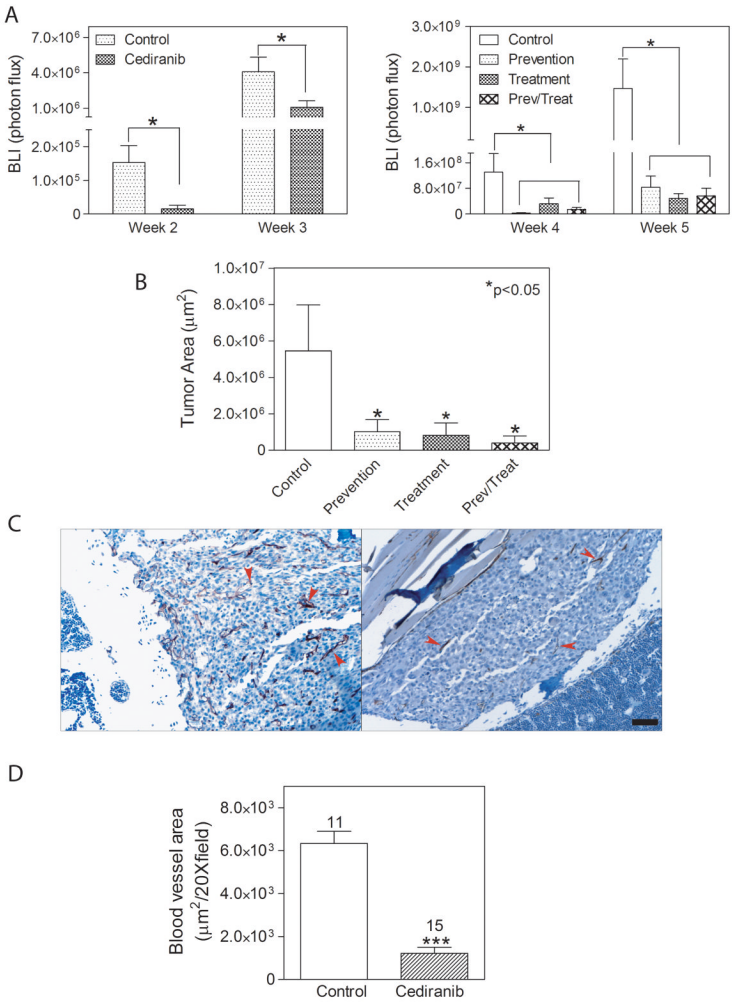

Figure 6.

Cediranib inhibited the development and progression of bone metastases. A. Bone tumor burdens were measured by BLI at weeks 2 and 3 (left panel), and at weeks 4 and 5 (right panel, note scale differences). * $p<0.05$; n=9-10. B. Histomorphometric analysis of bone metastases on H&E stained sections. * $p<0.05$, n=9-10. C. CD34 stains of endothelial cells in bone metastases from representative control and Cediranib treated mice. D. Quantification of blood vessel area on CD34 stained sections. *** $p<0.001$. Numbers indicate the bones analyzed in each group.

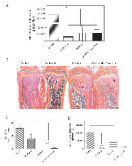

Figure 7.
Cediranib had similar efficacy as Zometa in inhibiting bone metastases. A. Bone tumor burden measured by BLI in each group. * $p<0.05$, n=9-11 B. Representative H&E orange G stained sections of proximal tibia from each group. T: tumor. C. Number of bone lesions quantified on X-rays. * $p<0.05$, ** $p<0.01$, n=9-11. D. Brain tumor burden quantified by BLI on week 5. ** $p<0.01$.